

Exponential Stabilization of a Class of Underactuated Mechanical Systems using Dynamic Surface Control

Nadeem Qaiser, Naeem Iqbal, Amir Hussain, and Naeem Qaiser

Abstract: This paper proposes a simpler solution to the stabilization problem of a special class of nonlinear underactuated mechanical systems which includes widely studied benchmark systems like Inertia Wheel Pendulum, TORA and Acrobot. Complex internal dynamics and lack of exact feedback linearizability of these systems makes design of control law a challenging task. Stabilization of these systems has been achieved using Energy Shaping and damping injection and Backstepping technique. Former results in hybrid or switching architectures that make stability analysis complicated whereas use of backstepping some times requires closed form explicit solutions of highly nonlinear equations resulting from partial feedback linearization. It also exhibits the phenomenon of explosions of terms resulting in a highly complicated control law. Exploiting recently introduced Dynamic Surface Control technique and using control Lyapunov function method, a novel nonlinear controller design is presented as a solution to these problems. The stability of the closed loop system is analyzed by exploiting its two-time scale nature and applying concepts from Singular Perturbation Theory. The design procedure is shown to be simpler and more intuitive than existing designs. Design has been applied to important benchmark systems belonging to the class demonstrating controller design simplicity. Advantages over conventional Energy Shaping and Backstepping controllers are analyzed theoretically and performance is verified using numerical simulations.

Keywords: Dynamic surface control, integrator backstepping, nonlinear control, underactuated mechanical systems.

1. INTRODUCTION

Study and control of the dynamics of Underactuated Mechanical Systems has been an active research area. These arise in a variety of applications including mobile Robots, underwater/surface vehicles and spacecrafts, see [1] and references therein. Underactuated Mechanical Systems are control systems with fewer actuators (i.e., controls) than configuration variables or degrees of freedom. The class we consider comprises mechanical systems with

two degrees of freedom with an inertia matrix that is independent of unactuated variable. Important examples include, Inertia Wheel Pendulum (IWP), Translational Oscillator with Rotational Actuator (TORA) and the Acrobot, in increasing order of dynamics complexity.

First choice in stabilization techniques, for nonlinear systems, is to use linearized/pseudo-linearized models and gain scheduling controllers. This proves inefficient for the case as vector field of closed-loop system vanishes at equilibrium points making the system sluggish. On the other hand exact feedback linearization for such systems is also not possible. However partial feedback linearization can be applied that reduces the system to cascade normal forms [2]. The structure of this form allows application of existing control design methods like Energy shaping techniques and Integrator Back-Stepping (IBS), [1,3-5]. In energy-based techniques, for instance in [3], a supervisory hybrid/switching control strategy is applied to asymptotic stabilization of the system. First, a passivity-based controller [4] forces the system near to the desired equilibrium point. Then, a balancing controller, obtained by Jacobian linearization or (local) exact feedback linearization stabilizes the system at that equilibrium point.

Manuscript received November 21, 2006; revised March 28, 2007; accepted July 6, 2007. Recommended by Editorial Board member Dong Hwan Kim under the direction of Editor Jae Weon Choi. This work was supported by the Higher Education Commission of Pakistan. The authors like to acknowledge the support of Higher Education Commission of Pakistan for funding this research and providing excellent online literature availability.

Nadeem Qaiser and Naeem Iqbal are with the Dept. of Electrical Engineering, Naeem Qaiser is with the Dept. of Computer Science and Information Technology, Pakistan Institute of Engineering and Applied Sciences Islamabad, Pakistan (e-mails: nadeem.qaiser@gmail.com, naeem.iqbal@pieas.edu.pk, naeem.qaiser@gmail.com).

Amir Hussain is with Dept. of Computer Science and Mathematics, University of Sterling, Scotland, U.K. (e-mail: a.hussain@cs.stir.ac.uk).

To avoid supervisory/switching controllers IBS based design have been applied successfully. IBS, based on results obtained by Sontag and Sussman [5], is a powerful step-by-step design tool. In such designs a stabilizing controller is first designed for the nonlinear part (reduced system) of the cascade and then assuming the states of linearized part as virtual inputs IBS is used to complete design, theoretically. Backstepping suffers not only the problem of “explosion of terms” but also requires certain system functions to be C^r [6]. Besides some times the control law for the reduced systems requires explicit solution of highly nonlinear equations, which complicates the design even if not denying it at all. The control law obtained through a cumbersome design procedure is usually very complicated. Multiple Sliding Surfaces (MSS) control [6], a procedure similar to integrator backstepping, avoids this phenomenon but falls short of integrator backstepping in terms of theoretical rigor, as the need for analytical differentiation is pushed to a numerical one.

Concept of Dynamic Surface Control (DSC), a dynamic extension to MSS, introduced by Swaroop *et al.* [7] resolves these issues by using low pass filters. It addresses not only the issue of “explosion of terms” associated with IBS, but also solves the problem of finding i th state reference (desired) trajectory derivatives numerically, for the MSS scheme. It is simple, more intuitive and applies to a more general class of systems as compared to the MSS scheme in Won and Hedrick [6] as the requirement on nonlinear function is to be C^1 only. More exotic methods like fuzzy controllers [8] and neural networks based solutions have also been reported but we are interested in classical nonlinear techniques only.

Exploiting DSC a controller design scheme is presented that addresses not only the problems highlighted but also gives a single simple design algorithm for the whole class. The design uses DSC technique to track the required stabilization function for the unstable zero dynamics instead of IBS. The design procedure and control law is simpler than IBS design and doesn't require a supervisory controller like the one by Spong *et al.* [3] making the architecture simple. Stability has been analyzed using concepts from singular perturbation theory. The scheme has been successfully used to design controllers for benchmark nonlinear systems like IWP, TORA and the Acrobot, demonstrating the design method simplicity that also results in a less complicated control law.

The paper starts formally with Section 2, containing the general dynamical model for our special class. Here necessary coordinate transformations are also given, as the dynamic model is not in a control design amenable form. Controller design strategy and procedure appear in Section 3. Section 4 hosts

detailed stability discussion. Section 5 presents application examples with simulation results comparing controller performance to existing designs followed by brief concluding remarks in Section 6.

2. DYNAMICAL MODEL

Dynamic model of two degrees of freedom underactuated mechanical systems can be obtained by using Euler Lagrange method [9]. The Lagrangian for a simple mechanical system for mentioned class is given as

$$L(q, \dot{q}) = \frac{1}{2} \dot{q}^T M(q_2) \dot{q} - V(q), \quad (1)$$

where $q = [q_1 \ q_2]^T$, (q, \dot{q}) are generalized coordinates and quasi velocities, $M(q_2)$ the inertia matrix and $V(q)$ is the potential energy function. For our special class note that $M(q_2)$ is independent of q_1 that is in fact the unactuated configuration variable for our modelling scheme. This property is referred to as kinetic symmetry with respect to q_1 in our case. Using the Lagrangian of the system, equations of motion can be found by

$$\frac{d}{dt} \frac{\partial L}{\partial \dot{q}} - \frac{\partial L}{\partial q} = Q(q)u \quad (2)$$

given as

$$\begin{bmatrix} m_{11} & m_{12} \\ m_{21} & m_{22} \end{bmatrix} \begin{bmatrix} \ddot{q}_1 \\ \ddot{q}_2 \end{bmatrix} + \begin{bmatrix} h_1 + \phi_1 \\ h_1 + \phi_1 \end{bmatrix} = \begin{bmatrix} 0 \\ \tau \end{bmatrix}. \quad (3)$$

The state space model for these systems is unsuitable for direct application of DSC [7] for not being in strict feedback form. Feedback Linearization employs a change of control and coordinate transformation, which leaves the system dynamics linear or at least partially linear, more amenable to control [2]. Different coordinate transformations have been used for benchmark systems belonging to this class for instance [3,10,11]. We prefer [11] that exploits structural properties and uses Collocated Partial Feedback Linearization, Spong [12]. Based on Theorem 1 [11] the following change of coordinates and invertible change of control input [12]

$$q_r = q_1 + \gamma(q_2), \quad (4)$$

$$p_r = m_{11}(q_2)p_1 + m_{12}(q_2)p_2, \quad (4)$$

$$\tau = \alpha(q_2)u + \beta(q, \dot{q}), \quad (5)$$

where

$$\gamma(q_2) = \int_0^{q_2} \frac{m_{12}(s)}{m_{11}(s)} ds \quad \text{and}$$

$$g(q_r, q_2) = - \left[D_{q_1} V(q_1, q_2) \right]_{q_1=q_r-\gamma(q_2)}$$

transforms the dynamics in (3) to a cascade nonlinear system in strict feedback form.

$$\dot{q}_r = p_r / m_{11}(q_2), \quad (6)$$

$$\dot{p}_r = g_r(q_r, q_2),$$

$$\dot{q}_2 = p_2, \quad (7)$$

$$\dot{p}_2 = u.$$

Remark 1: System after coordinate transformation is a cascaded interconnection of a nonlinear (core or reduced) subsystem and a linear (double integrator) subsystem.

Remark 2: After transformation the obtained form is amenable to several control design techniques. Normally backstepping or energy based techniques are applied after this stage.

3. CONTROLLER DESIGN

Although the transformed system is in strict feedback form but DSC technique is not applicable in usual fashion as the core system is non-affine in control. Thus first assuming q_2 as the virtual input a stabilization function is found for the core subsystem. Afterwards DSC technique is used to design u forcing q_2 to track the required stabilization function, ultimately stabilizing the total system. DSC is chosen as it has not only nice trajectory tracking feature with arbitrarily small bounded error but it also doesn't exhibit the phenomenon of explosion of terms associated with IBS.

3.1. Core subsystem controller design

The equations of the core systems are often highly nonlinear and the virtual input appears in a very complicated manner. However assuming $q_2 = v$ as a virtual control input, existence of a static feedback for (6) in the explicit form

$$v(q_r, p_r) = \alpha(q_r) - a\sigma(c_1 q_r + c_2 p_r) \quad (8)$$

is guaranteed by Theorem 3.2 [13], which globally asymptotically stabilizes the core system. Here $\alpha(q_r)$ is a smooth function that satisfies

$$g_r(q_r, \alpha(q_r)) = 0, \quad \alpha(0) = 0. \quad (9)$$

However using control Lyapunov Functions simpler control laws do exist for stabilization of reduced systems for certain cases as is demonstrated for cases of IWP and TORA in example section.

Remark 3: Normally backstepping is recommended to complete the design, [13]. Theoretically

the procedure yields a static feedback that guarantees stability of total system. Whereas practically for subsequent design it requires derivatives of (9). This obviously demands availability of explicit solution of (9) in closed form during design. For systems having highly complicated dynamics, for instance, like that of the Acrobot it is very hard to find such solutions even by using symbolic computing engines. Implicit solutions can be found [13]; requiring inversions by exotic methods like lookup tables, neural networks, splines, or other curve fitting approaches. However solutions provided by these are useless for backstepping for being numerical in nature.

One of the advantages of presented scheme is that it doesn't require this solution necessarily to be available in closed form during design and thus $\alpha(q_r)$ can be calculated numerically online and used.

3.2. Outer subsystem controller design

To stabilize (6) q_2 is required to follow the trajectory given as

$$\bar{q}_{2d} := v(q_r, p_r). \quad (10)$$

Applying DSC technique we design a control law that forces the linear system to generate the required stabilization function. Theorem for Boundedness of Tracking Error Using DSC for Lipschitz Systems by Swaroop *et al.* [7] lists necessary requirements for applications DSC technique. It's trivial to verify that required assumptions are satisfied by (7) regarding the system which is in strict feedback form with $f \in C^1$, and by (10) regarding the trajectory as $\alpha(q_r)$ is smooth and $\sigma(c_1 q_r + c_2 p_r)$ is a sigmoidal function.

3.2.1 Design procedure

Let the error in generation of stabilization function be S_1

$$S_1 := q_2 - q_{2d}, \quad (11)$$

$$\dot{S}_1 = \dot{q}_2 - \dot{q}_{2d} = p_2 - \dot{q}_{2d}. \quad (12)$$

Assuming p_2 as next virtual input \bar{p}_3 is chosen to drive S_1 to zero.

$$\bar{p}_2 = -K_1 S_1 + \dot{q}_{2d} \quad (K_1 > 0) \quad (13)$$

Notice that the direct calculation of $\dot{q}_{2d}(t)$ required at this step by the conventional backstepping design procedure requires availability of q_{2d} in analytical form, calculation of which has already been seen as a very difficult task. Even if it is available it leads to complexity due to "explosion of terms". Motivated by DSC technique [7] a low pass filter with

small positive time constant τ_q given as following is used here

$$\tau_q \dot{q}_{2d}(t) + q_{2d}(t) = \bar{q}_{2d}, \quad q_{2d}(0) = \bar{q}_{2d}(0), \quad (14)$$

where $q_{2d}(t)$ and $\dot{q}_{2d}(t)$ are obtained by online filtering of \bar{q}_{2d}

$$\dot{q}_{2d}(t) = \frac{\bar{q}_{2d} - q_{2d}(t)}{\tau_q}. \quad (15)$$

Define the second surface as

$$S_2 := p_2 - p_{2d}, \quad (16)$$

$$\dot{S}_2 = \dot{p}_2 - \dot{p}_{2d} = u - \dot{p}_{2d}. \quad (17)$$

Control input u is designed to derive S_2 to zero

$$u = -K_2 S_2 + \dot{p}_{2d}, \quad K_2 > 0. \quad (18)$$

Another low pass filter with small positive time constant τ_p given as following is used here

$$\tau_p \dot{p}_{2d}(t) + p_{2d}(t) = \bar{p}_{2d}, \quad p_{2d}(0) = \bar{p}_{2d}(0), \quad (19)$$

where $p_{2d}(t)$ and $\dot{p}_{2d}(t)$ are obtained by filtering \bar{p}_{2d}

$$\dot{p}_{2d}(t) = \frac{\bar{p}_{2d}(t) - p_{2d}(t)}{\tau_p}, \quad (20)$$

which completes the design and

$$u = -K_2 S_2 + \frac{\bar{p}_{2d}(t) - p_{2d}(t)}{\tau_p}. \quad (21)$$

Substituting (21) in (5) gives the required τ .

3.3. Controller parameters

As obvious from design K_i can be set moderately high for faster convergence rates. Filter time constants control boundary layer error and hence must be set as low as possible. However physical component values and actuator saturation must be kept in mind as smaller values increase control effort peaks and make the control signal noisy. Average control effort and rise time can be tuned by adjusting c_1 and transients damping can be enhanced using c_2 .

It is interesting to see that during design the control law and its derivative are never required in their analytical forms during design. This solves the issue of finding closed form solution for (9) which are otherwise available easily using numerical techniques. The procedure also circumvents the issue of explosions of term effectively thus the resulting control law is simpler with easy implementation.

Besides it gives a single controller design algorithm for whole of the class, as sufficient conditions, found in next section are not very restrictive. A comparison to existing designs in [3,10,13] reveals the ease of design and simplicity of obtained control law.

4. STABILITY ANALYSIS

Although core is GAS for the virtual input defined as (8) and errors in virtual control are removed exponentially but it's not sufficient to prove stability as it ignores filter dynamics. Addition of low pass filters makes things more complicated and it's hard to find a simple Lyapunov function to prove stability using classical techniques. The MSS controller doesn't follow an independent trajectory thus Theorem for Boundedness of Tracking Error Using DSC for Lipschitz Systems by Swaroop *et al.* [7], also, cannot be used directly to infer the stability of the system.

Fortunately the filter time constants can be set arbitrarily low. By exploiting this we show that for sufficiently small filter time constants the system shows two-time scale nature and can be modelled as a singularly perturbed system. Khalil [14] and references therein provide a good account of the theory of singularly perturbed system and terminology adopted in the following discussion.

Our main result summarized as proof of given proposition and following theorem analyzes closed loop system stability by examining the reduced and boundary layer models, obtained by using concepts from singular perturbation theory.

Proposition 3.3.1: The augmented error dynamics formed by closed loop system with controller designed and low pass filter equations can be written as a standard singularly perturbed model given as following

$$\dot{x} = f(x, z), \quad (22)$$

$$\varepsilon \dot{z} = g(x, z, \varepsilon), \quad (23)$$

where f and g are continuously differentiable in their arguments for $(x, z, \varepsilon) \in D_x \times D_z \times [0, \varepsilon_0]$, $D_x \subset \mathbb{R}^4$, $D_z \subset \mathbb{R}^2$ and ε is a small positive parameter.

Proof: Let the boundary layer errors are given as

$$z_1 := q_{2d} - \bar{q}_{2d}, \quad (24)$$

$$z_2 := p_{2d} - \bar{p}_{2d}. \quad (25)$$

Thus From (15) and (20)

$$\dot{q}_{2d}(t) = \frac{\bar{q}_{2d} - q_{2d}(t)}{\tau_q} = -\frac{z_1}{\tau_q}, \quad (26)$$

$$\dot{p}_{2d}(t) = \frac{\bar{p}_{2d}(t) - p_{2d}(t)}{\tau_p} = -\frac{z_2}{\tau_p}. \quad (27)$$

Thus

$$p_2 = p_{2d} + S_2 + z_2, \quad (28)$$

$$q_2 = q_{2d} + S_1 + z_1. \quad (29)$$

Boundary layer error dynamics can be found as following

$$\dot{z}_1 = \dot{q}_{2d} - \dot{\bar{q}}_{2d} = -\frac{z_1}{\tau_q} - B_1(S, p_r, q_r, z), \quad (30)$$

$$\dot{z}_2 = \dot{p}_{2d} - \dot{\bar{p}}_{2d} = -\frac{z_2}{\tau_p} - B_2(S, p_r, q_r, z).$$

After substitutions and some algebraic manipulations we can write the augmented error dynamics as

$$\dot{q}_r = p_r / m_{11}(v, S_1, z_1), \quad (31)$$

$$\dot{p}_r = g_r(q_r, v, S_1, z_1),$$

$$\dot{S}_1 = -K_1 S_1 + S_2 + z_2, \quad (32)$$

$$\dot{S}_2 = -K_2 S_2,$$

$$\dot{z}_1 = -\frac{z_1}{\tau_q} - B_1(S, p_r, q_r, z), \quad (33)$$

$$\dot{z}_2 = -\frac{z_2}{\tau_p} - B_2(S, p_r, q_r, z),$$

where $B_i(\cdot)$ is an appropriate continuous function. Filter time constants $\tau_{q,p}$ can be set arbitrarily small and (33) has an isolated real root when $\tau_{q,p} = 0$. Thus after renaming variables as $x = [q_r, p_r, S_1, S_2]^T$, $z = [z_1, z_2]^T$ and $\varepsilon = \tau_q = \tau_p$, the composite system can be modelled as a singularly perturbed system, written in standard form as in (22), (23). \square

Stability of these augmented error dynamics implies the stability of the closed loop system, which we prove in following theorem.

Theorem 3.3.1: Lets assume that the following holds for $f(q_r, v(q_r, p_r), 0, 0)$ in (31).

-H1: $f(0, 0, 0, 0) = 0$.

-H2: $f(q_r, v(q_r, p_r), 0, 0)$ is continuously differentiable with bounded derivatives up to the second order in $x \in B_\rho$.

-H3: Linearization $A_{11} := [\partial f(q_r, v(q_r, p_r), 0, 0) / \partial (q_r, p_r)](0)$ is Hurwitz.

-H4: $g(0, 0, 0) = 0$, $g(\cdot)$ and its partial derivatives up to second order are bounded in $z \in B_\rho$.

Then for the closed loop system formed by (6), (7) and the controller designed in Sections 3.1 and 3.2 with appropriate choices of $K_1, K_2, \tau_p, \tau_q, a, c_1$, and

c_2 there exists $\varepsilon^* > 0$ such that for all $\varepsilon < \varepsilon^*$, the origin of the augmented error dynamics (22), (23) is exponentially stable.

Proof: We exploit the two-time scale nature of the system (22), (23) and an isolated root $z := h(x) = 0$, is found as solution of $0 = g(x, z, 0)$. Thus the quasi steady state of z is at origin and the reduced system $\dot{x} = f(x, h(x))$ is given as following.

$$\dot{x}_1 = x_2 / m_{11}(v(x_1, x_2), x_3), \quad (34)$$

$$\dot{x}_2 = g(x_1, v(x_1, x_2), x_3),$$

$$\begin{bmatrix} \dot{x}_3 \\ \dot{x}_4 \end{bmatrix} = \begin{bmatrix} -K_1 & 1 \\ 0 & -K_2 \end{bmatrix} \begin{bmatrix} x_3 \\ x_4 \end{bmatrix} := A_{22} \begin{bmatrix} x_3 \\ x_4 \end{bmatrix}. \quad (35)$$

Linearization of this system around origin can be written as

$$\dot{x} = Ax, \quad (36)$$

where $A = \begin{bmatrix} A_{11} & A_{12} \\ 0 & A_{22} \end{bmatrix}$ and A_{12} defines appropriate

interconnection terms. A is Hurwitz due to its special block diagonal structure, by H3 and by definition of A_{22} . Combining this with H2 and using Lyapunov indirect method, this shows exponential stability of origin of (34)-(35), Theorem 4.15 [14]. By Theorem 4.14 [14], there is a Lyapunov function $V(x)$ for the reduced system that satisfies for some positive constants c_i for $x \in B_{r_0}$ where $r_0 < r$

$$c_1 \|x\|^2 \leq V(x) \leq c_2 \|x\|^2, \quad (37)$$

$$\frac{\partial V}{\partial x} f(x, h(x)) \leq -c_3 \|x\|^2, \quad (38)$$

$$\left\| \frac{\partial V}{\partial x} \right\| \leq c_4 \|x\|. \quad (39)$$

Equation (23) can be rewritten as

$$\varepsilon \dot{z} = g(x, z, \varepsilon) = -A_z z + \varepsilon p(x, z), \quad (40)$$

where $A_z = \begin{bmatrix} 1 & 0 \\ 0 & 1 \end{bmatrix}$.

Further applying a change of time scale to (40) as $\varepsilon \frac{dz}{dt} = \frac{dz}{dt_s}$ or $\frac{dt_s}{dt} = \frac{1}{\varepsilon}$ and setting $\varepsilon = 0$ yields the boundary layer system given as

$$\frac{dz}{dt_s} = g(x, z, 0) = -A_z z. \quad (41)$$

Due to simple structure of low pass filters it is not only independent of x but is also exponentially stable as A_z is Hurwitz. Treating x as a frozen parameter,

by Lemma 9.8 [14], there is a Lyapunov function $W(z)$ for the boundary layer system that satisfies

$$b_1 \|z\|^2 \leq W(z) \leq b_2 \|z\|^2, \quad (42)$$

$$\frac{\partial W}{\partial z} g(x, z, 0) \leq -b_3 \|z\|^2. \quad (43)$$

From H1 and H4 it follows that f and g are Lipschitz in ε and suppose the following estimates hold

$$\|f(x, z) - f(x, 0)\| \leq L_1 \|x\|, \quad (44)$$

$$\|f(x, 0)\| \leq L_2 \|x\|. \quad (45)$$

We use

$$v(x, z) = V(x) + W(z) \quad (46)$$

as a composite Lyapunov function candidate for the system (22), (23). The derivative of $v(x, z)$ along the trajectories of the system is given as following

$$\begin{aligned} \dot{v}(x, z) &= \frac{\partial V}{\partial x} f(x, z) + \frac{1}{\varepsilon} \frac{\partial W}{\partial z} [-A_z z + \varepsilon p(x, z)] \\ &= \frac{\partial V}{\partial x} f(x, 0) + \frac{\partial V}{\partial x} [f(x, z) - f(x, 0)] \\ &\quad - \frac{1}{\varepsilon} \frac{\partial W}{\partial z} A_z z + \frac{\partial W}{\partial z} p(x, z). \end{aligned} \quad (47)$$

Using the estimates (44), (45) and properties (37)-(39), (42), (43) of $V(x)$ and $W(z)$ it can be verified that following inequality holds

$$\begin{aligned} \dot{v}(x, z) &\leq -c_3 \|x\|^2 + c_4 L_1 \|x\| \|z\| - \frac{1}{\varepsilon} z^T z - b_3 \|z\|^2 \\ &= - \begin{bmatrix} \|x\| \\ \|z\| \end{bmatrix}^T \begin{bmatrix} c_3 & -c_4 L_1 / 2 \\ -c_4 L_1 / 2 & (1/\varepsilon) + b_3 \end{bmatrix} \begin{bmatrix} \|x\| \\ \|z\| \end{bmatrix} \\ &= - \begin{bmatrix} \|x\| \\ \|z\| \end{bmatrix}^T M \begin{bmatrix} \|x\| \\ \|z\| \end{bmatrix}, \end{aligned} \quad (48)$$

where $c_3 > 0$ and to make M positive definite we need $c_3((1/\varepsilon) + b_3) - (c_4 L_1 / 2)^2 > 0$. As we can choose ε arbitrarily small thus there exists $\varepsilon^* > 0$ such that for all $\varepsilon < \varepsilon^*$, we have

$$\dot{v}(x, z) \leq -2\gamma v, \quad (49)$$

$$v(x(t), z(t)) \leq \exp[-2\gamma t] v(x(0), z(0)), \gamma > 0, \quad (50)$$

and from properties of $V(x)$ and $W(z)$

$$\begin{bmatrix} \|x(t)\| \\ \|z(t)\| \end{bmatrix} \leq K_1 \exp[-\gamma t] \begin{bmatrix} \|x(0)\| \\ \|z(0)\| \end{bmatrix}, \quad (51)$$

which completes the proof. \square

Remark 4: All the requirements listed as H1, H2, H3, H4 and estimates (44), (45) are not very restrictive and it is trivial to verify that these are satisfied by benchmark systems used in examples section.

5. ILLUSTRATIVE EXAMPLES

Design algorithm presented in Section 3 has been successfully applied to synthesize controllers for benchmark systems belonging to our special class of under actuated mechanical systems. These include TORA [15], IWP and Acrobot. The Lagrangian models of these benchmark systems possess kinetic symmetry with respect to q_1 in spite of possessing no symmetry in classical sense [11]. This makes them perfect candidates for the class defined in Section 2. It is interesting to note that our design gives a single algorithm for different systems belonging to the mentioned class, which is a great advantage if we see the variety in existing design for different system. It is trivial to verify that reduced systems of the examples satisfy the requirements listed in Section 4.

5.1. TORA

TORA first introduced by Wan *et al.* [10], has been extensively used as a test bed for nonlinear controllers for cascade systems, mainly for passivity based approaches [16]. Global stabilization of TORA system using Integrator Backstepping procedure (IBS) has been known due to Wan *et al.* [10], Raza [17].

The TORA system as depicted in Fig. 1 consists of a translational oscillating platform, which is controlled via a rotational eccentric mass. Model of TORA after applying coordinates transformation given in Section 2 the reduced system is given as

$$\begin{aligned} \dot{q}_r &= m p_r, \\ \dot{p}_r &= -k_1 q_r + e \sin(q_2). \end{aligned} \quad (52)$$

It satisfies all the conditions listed for stability in

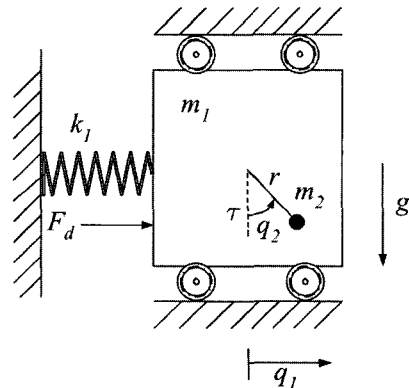


Fig. 1. The TORA system.

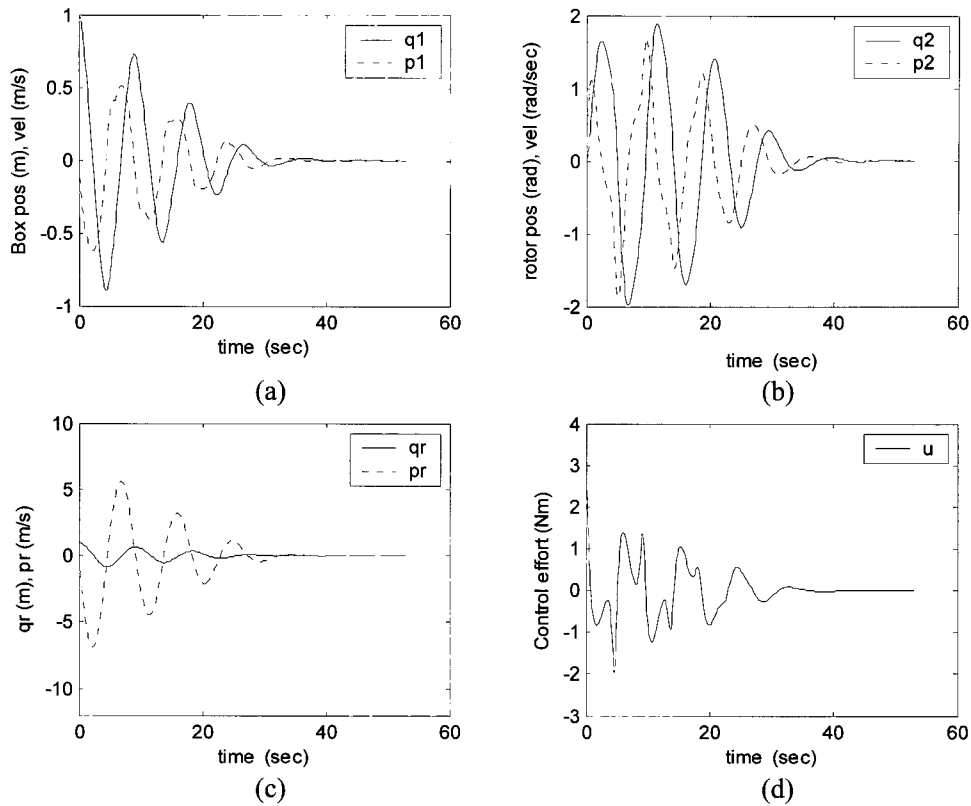


Fig. 2. (a) Box position and velocity (b) Rotor position and velocity (c) Core system trajectories (d) Control effort.

Section 4. Assuming q_2 as an input for (52) and taking $V_0(q_r, p_r) = \frac{1}{2}(k_1 q_r^2 + m p_r^2)$ as a Lyapunov function candidate, a control is found such that \dot{V}_0 is rendered negative definite. Trying $q_2 := \alpha(p_r) = -a \tan^{-1}(c_1 p_r)$.

$$\dot{V}_0 = -\varepsilon m p_r \sin(a \tan^{-1}(c_1 p_r)) \leq 0, \quad (53)$$

where $0 < a < \frac{\pi}{2}$ and $c_1 > 0$.

This is negative semi definite but is sufficient to show Global Asymptotic Stability (GAS) of the origin of (52) with help of LaSalle's invariance. For a fair performance comparison the initial conditions and parameters used for TORA have been principle. Let the largest invariant set where all solutions converge is

$$\Omega = \{[p_r, q_r] \in R^2 : \dot{V}(p_r, q_r) = 0\}.$$

This is $p_r = 0$ and from (52)

$$p_r = 0 \Rightarrow \dot{p}_r = 0 \Rightarrow q_r = 0.$$

Thus $\Omega = \{0\}$. The outer subsystem is designed as described in Section 3 with control law given as (21).

A comparison to design of Wan *et al.* [10] reveals

the ease of design and simplicity of obtained control law. System parameters are kept same as by Reza [17], i.e., $m_1 = 10$, $m_2 = 1$, $k_1 = 5$, $r = 1$, $I = 1$. Following controller parameters were used for simulations. $a = 1.15$, $c_1 = 0.5$, $K_1 = 1.2$, $K_2 = 2.5$, $\tau_{p,q} = 1$. The controller effectively damps translational vibrations of cart and brings rotor to origin in reasonable time, Fig. 2(a), 2(b), and 2(c). The stabilization is more aggressive than Reza [17]. However initial control effort peaks are higher in this case, Fig. 2(d).

5.2. IWP

IWP first introduced by Spong *et al.* [3], is a Benchmark nonlinear UMS, used mainly for Energy Shaping and Damping Injection based approaches [3].

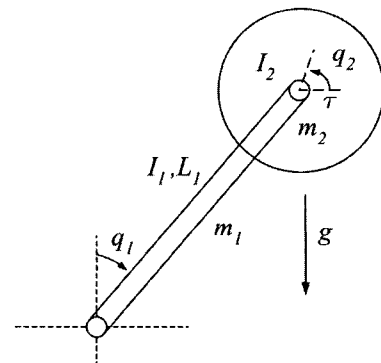


Fig. 3. The inertia wheel pendulum system.

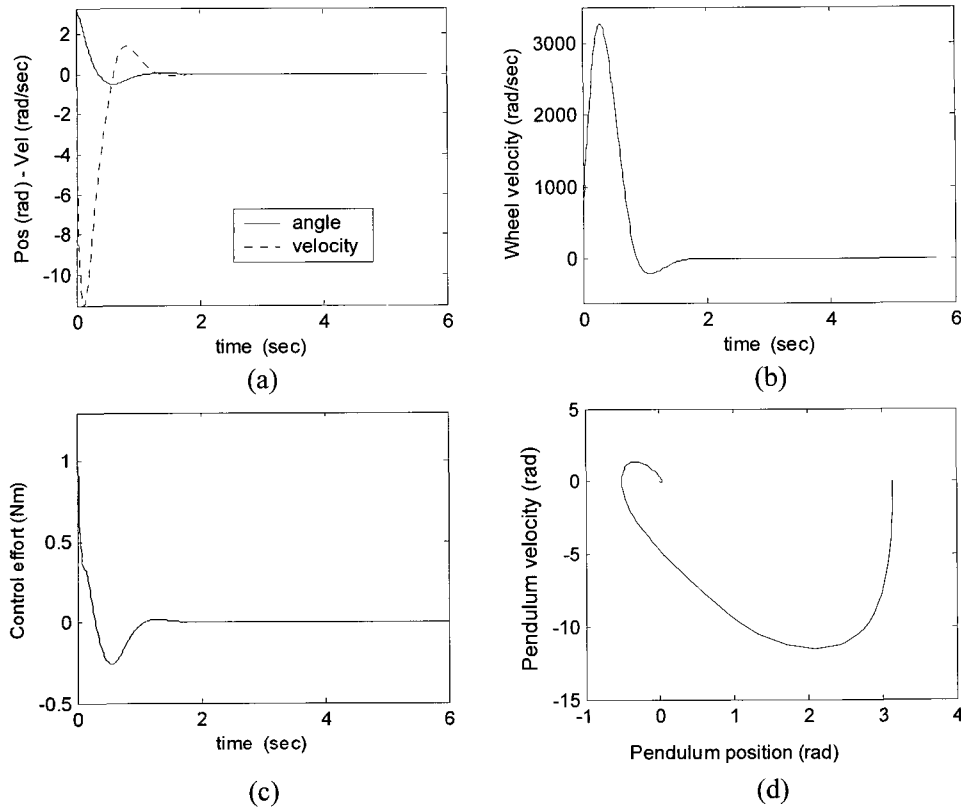


Fig. 4. (a) Pendulum position and velocity (b) Wheel velocity (c) Control effort (d) Phase portrait.

The IWP as illustrated in Fig. 3 is a planar inverted pendulum with a rotating wheel on the end. The joint on the base is unactuated thus the pendulum is to be controlled through wheel rotation.

The controller task is to stabilize the pendulum in its upright equilibrium position while the wheel stops rotating. The specific angle of rotation of the wheel is not important. In [3], a supervisory hybrid/switching control strategy is applied for asymptotic stabilization of the inertia-wheel pendulum around its upright equilibrium point. First, a passivity-based controller [4] swings up the pendulum. Then, a balancing controller, obtained by Jacobian linearization or (local) exact feedback linearization stabilizes the pendulum around its upright position.

Transformed dynamical model of IWP after applying coordinates transformation [17] is given as

$$\begin{aligned} \dot{z}_1 &= w \sin(z_2), \\ \dot{z}_2 &= \frac{1}{m_{11}} z_1 - \frac{m_{12}}{m_{11}} z_3, \\ \dot{z}_3 &= u. \end{aligned} \quad (54)$$

Spong *et al.* [3] using a standard method from [2] perform Feedback linearization of the system for controller design. Reza [17] also applies further change of coordinates and control to (54).

Besides IBS design still requires propagation of derivatives during design. Our design approach

doesn't require any further transformations before application of same simple design algorithm. For

obvious reasons $\bar{z}_3 = \frac{m_{11}}{m_{12}} (K_1 S_1 + \frac{1}{m_{11}} z_1 - \dot{z}_{2d})$ in (13).

A comparison to existing design methods for instance [3] and [17] reveals the ease of design and simplicity of obtained control law. For fair performance comparisons Reza [17] uses same system parameters as Spong [3], and so do we i.e., $m_1 = 4.83 \times 10^{-3}$, $m_{12} = m_{21} = m_{22} = 32 \times 10^{-6}$, and $w = 379.26 \times 10^{-3}$. Following controller parameters were used for simulations $a = \pi/2$, $c = 9$, $K_1 = 4$, $K_2 = 6$, and $\tau_{p,q} = 0.035$.

As depicted in Fig. 4 nonlinear controller aggressively stabilizes pendulum from its downward stable equilibrium point to its upright unstable equilibrium point with negligible transients, while wheel stops rotating. Swing up is faster than the design by Reza [17]. Design algorithm is simpler than the designs by Reza [17] that requires more coordinate transformations and IBS [2], which exhibits the phenomenon of explosion of terms. The structure is also simpler requiring no supervisory switching controller as Spong's design [3]. However initial control effort peaks are comparatively larger (1.4 Nm vs. 0.6 Nm by Reza) in this case.

5.3. Acrobot

Acrobot is a planar robot that mimics the human acrobat that hangs from a bar and tries to swing up to a perfectly balanced upside-down position with his/her hands still on the bar in Fig. 5.

The Acrobot, having a rich research past, first introduced and studied by Murray and Hauser [18], is a benchmark nonlinear under actuated mechanical system. The Acrobot has been a test bed mainly for Energy Shaping and Damping Injection based approaches. Normally a supervisory hybrid/switching control strategy is applied. Because of the large range of the motion the swing-up problem is highly nonlinear in nature, attracting attention of many control designers. Several solutions have been proposed ranging from Pseudo linearization techniques to more exotic like fuzzy controllers and use of neural networks.

The equations of motion for Acrobot are given as following

$$\begin{bmatrix} m_{11} & m_{12} \\ m_{21} & m_{22} \end{bmatrix} \begin{bmatrix} \ddot{q}_1 \\ \ddot{q}_2 \end{bmatrix} + \begin{bmatrix} h_1 + \phi_1 \\ h_1 + \phi_1 \end{bmatrix} = \begin{bmatrix} 0 \\ \tau \end{bmatrix}. \quad (55)$$

The element of Inertia matrix are given by

$$\begin{aligned} m_{11}(q_2) &= a + b \cos(q_2), \\ m_{12}(q_2) &= c + (b/2) \cos(q_2), \\ m_{22}(q_2) &= c. \end{aligned}$$

with

$$\begin{aligned} a &= m_1 l_1 + m_2 (L_1^2 + l_2^2) + I_1 + I_2, \\ b &= 2m_1 L_1 l_2, \\ c &= m_2 l_2^2 + I_2. \end{aligned}$$

There is no need for the definition of h_i and ϕ_i in design procedure; interested readers may find the same in [20]. After applying coordinate transformations mentioned in Section 2 the core system is written as (6) with

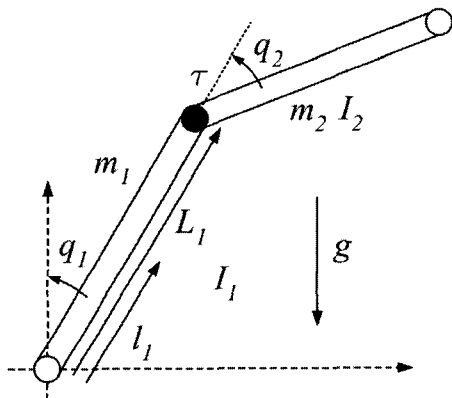


Fig. 5. The Acrobot.

$$\begin{aligned} g_r(q_r, q_2) &= (m_1 l_1 + m_2 L) g \sin(q_r - \gamma(q_2)) \\ &\quad + m_2 l_2 \sin(q_r - \gamma(q_2)) + \left(\frac{q_2}{2}\right) \end{aligned}$$

and

$$\gamma(q_2) = \frac{q_2}{2} + \left(\frac{2c - a}{\sqrt{a^2 - b^2}} \right) \arctan \left(\sqrt{\frac{a-b}{a+b}} \tan \left(\frac{q_2}{2} \right) \right).$$

Spong [20] proposes two distinct design algorithms for swing-up control. One design exploits unstable zero dynamics of the system for swing up while energy-pumping scheme is employed in the other. Global stabilization of Acrobot has also been suggested using Integrator Backstepping procedure (IBS) by Reza [17]. Former requires a supervisory control and later exhibits explosion of terms and requires the explicit solution of (9) in closed form. As demonstrated our presented scheme caters for both of the issues.

Control law given in (8) is used to stabilize the core system and the outer subsystem design follows steps given in Section 3 with control law given as (21).

Instead of a closed form solution for (9) our design allows us to use any numerical technique which is a great practical advantage. As implicit solutions are available for (9) a lookup table can also be used. However we prefer a numerical solution for the isolated root $\alpha(q_r)$ for precision reasons. The algorithm [19] employed uses a combination of bisection, secant, and inverse quadratic interpolation methods for fast convergence. The function $\alpha(q_r)$ can be approximated with a straight line. This approximation is used to calculate a suitable guess for the algorithm for faster convergence. For simulations nonlinear function $\gamma(q_2)$ has been constructed piecewise.

For an objective performance comparison we use the same system parameters as [17] namely: $m_1 = m_2 = 1$, $l_1, l_2 = 1$, and $I_1, I_2 = 1/3$. Following controller parameters were used for simulations $a = 1$, $c_1 = 3$, $c_2 = 1$, $K_1 = 5$, $K_2 = 10$, and $\tau_q = \tau_p = 0.07$. As depicted in Figs. 6 and 7 the nonlinear controller aggressively stabilizes Acrobot from both sets of initial conditions to its upright unstable equilibrium point. Stabilization is aggressive than [17].

6. CONCLUSIONS

The DSC technique has been exploited in a novel way to design a new controller for a special class of nonlinear underactuated mechanical systems. The model is brought to a cascade in strict feedback form before applying the modular design procedure. First a control Law is found for the nonlinear part of the

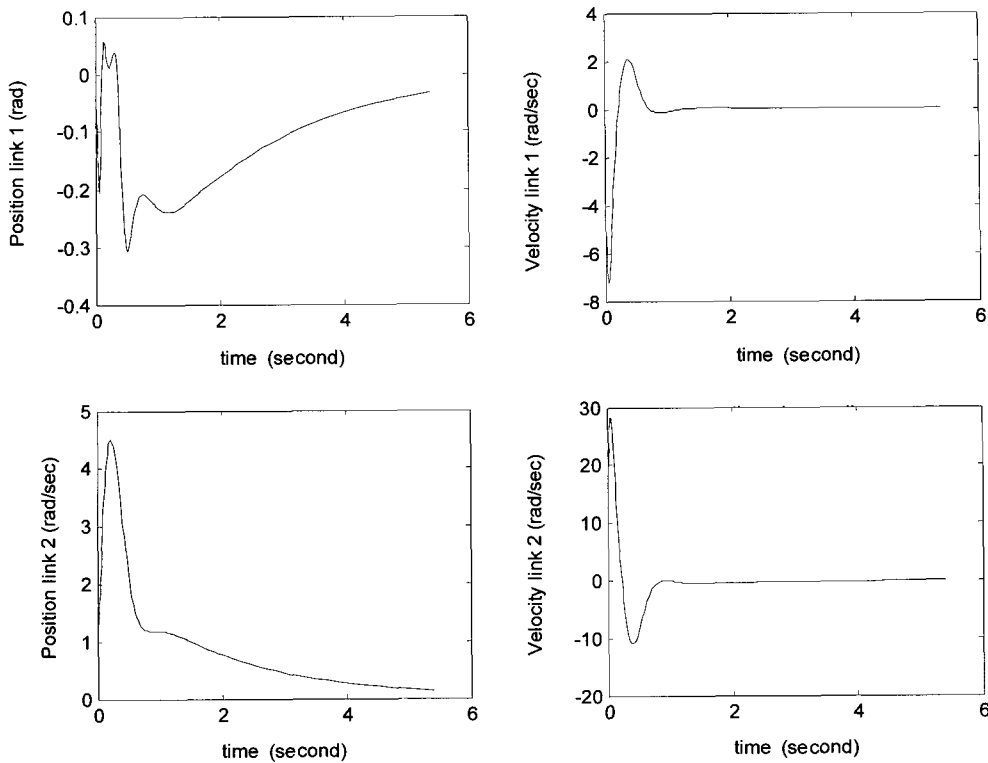


Fig. 6. Trajectory of (q_1, p_1, q_2, p_2) for the Acrobot with initial conditions $(\pi/3, 0, 0, 0)$.

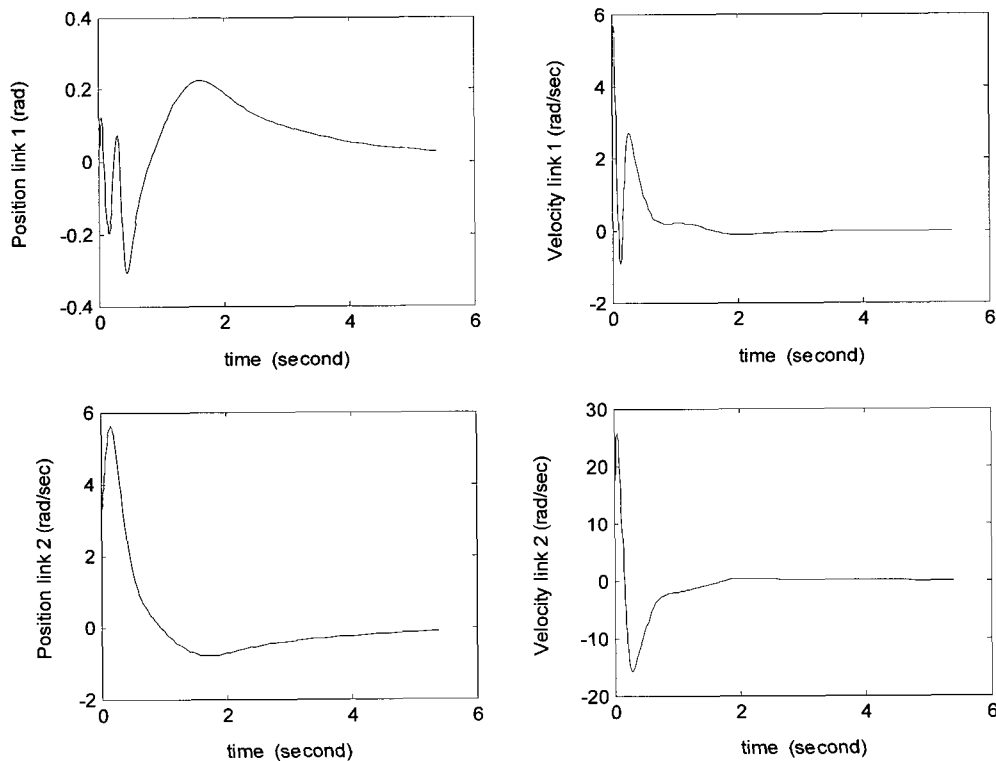


Fig. 7. Trajectory of (q_1, p_1, q_2, p_2) for the Acrobot with initial conditions $(0, 0, \pi, 0)$.

cascade, using control Lyapunov function method or any other suitable technique. The linear part, using DSC, is then forced to generate this control law. Stability of the system is analyzed using concepts

from singular perturbation theory with help of composite Lyapunov functions. Technique has been applied successfully to benchmark systems like TORA, IWP and Acrobot. Examples demonstrate how

the presented design gets rid of solving highly nonlinear equations, as in Acrobot example and phenomenon of explosion of terms in general. Design simplicity is demonstrated and controller performance is compared to existing designs using both theoretical and simulation studies. Some critical issues concerning the initial conditions of the system have also been studied numerically.

In conclusion, the proposed algorithm provides a very simple controller synthesis procedure that is applicable equally to whole class as compared to separate designs existing for different systems belonging to the same class. It requires fewer transformations and results in a less complicated control law.

The structure is also simpler requiring no supervisory switching controller. Simulation results show design achieves faster stabilization too. Future work includes investigation of the robustness of the controller. It is very important as the design procedure uses cancellation of derivatives that involve uncertain system parameters. It will be also interesting to investigate structural properties of the systems belonging to said class as this may help to simplify the control law for the core system.

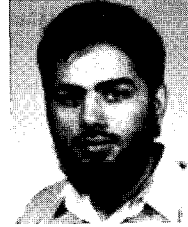
REFERENCES

- [1] M. W. Spong, "Underactuated mechanical systems," In B. Siciliano and K. P. Valavanis, editor, *Control Problems in Robotics and Automation*, SpringerVerlag, London, UK, 1997.
- [2] Alberto Isidori, *Nonlinear Control Systems*, 2nd edition, Springer-Verlag, Berlin, 1989.
- [3] M. W. Spong, P. Corke, and R. Lozano, "Nonlinear control of the inertia wheel pendulum," *Automatica*, vol. 37, pp. 1845-1851, 2001.
- [4] I. Fantoni, R. Lozano, and M. W. Spong, "Energy based control of the Pendubot," *IEEE Trans. on Automatic Control*, vol. 45, no. 4, pp. 725-729, 2000.
- [5] E. D. Sontag and H. J. Sussman, "Further comments on the stability of the angular velocity of a rigid body," *Systems and Control Letters*, vol. 12, pp. 213-217, 1988.
- [6] J. K. Hedrick and Y. Y. Yip, "Multiple sliding surface control: Theory and application," *Trans. ASME, Journal of Dynamic Systems, Measurement, and Control*, vol. 122, no. 4, pp. 586-593, 2000.
- [7] D. Swaroop, J. K. Hedrick, P. P. Yip, and J. C. Gerdes, "Dynamic surface control for a class of nonlinear systems," *IEEE Trans. on Automatic Control*, vol. 45, no. 11, pp. 1893-1899, Oct. 2000.
- [8] X. Lai, J.-H. She, Y. Ohya, and Z. Cai, "Fuzzy control strategy for acrobots combining model-free and model-based control," *IEE Proceedings-Control Theory & Applications*, vol. 146, no. 6, pp. 505-510, November 1999.
- [9] H. Goldstein, *Classical Mechanics*, 2nd edition, Addison Wesley, USA, 1981.
- [10] C. J. Wan, D. D. Bernstein, and T. V. Coppola, "Global stabilization of the oscillating eccentric rotor," *Proc. of the 33rd Decision & Control Conference*, Florida, USA, pp. 4024-4029, Dec. 1994.
- [11] R. Olfati-Saber, "Normal forms for underactuated mechanical systems with symmetry," *IEEE Trans. on Automatic Control*, vol. 47, no. 2, pp. 305-308, Feb. 2002.
- [12] M. W. Spong, "Energy based control of a class of under actuated mechanical systems," *Proc. of IFAC World Congress*, vol. F, pp. 431-435 July 1996.
- [13] R. Olfati-Saber, "Control of underactuated mechanical systems with two degrees of freedom and symmetry," *Proc. Amer. Control Conf.*, Chicago, IL, vol. 6, pp. 4092-4096, June 2000.
- [14] H. K. Khalil, *Nonlinear Systems*, 3rd edition, p. 165, pp. 423-460, Prentice-Hall, USA, 2000.
- [15] M. Jankovic, D. Fontaine, and P. V. Kokotovic, "TORA example: Cascade and passivity based control designs," *IEEE Trans. on Control System Technology*, vol. 34, no. 7, pp. 907-915, 1996.
- [16] R. Olfati-Saber, *Nonlinear Control of Under-actuated Mechanical Systems with Application to Robotics and Aerospace Vehicles*, Ph.D. Thesis, Department of Electrical Engineering and Computer Science, MIT, 2001.
- [17] R. M. Murray and J. Hauser, "A case study in approximate linearization: The Acrobot example," *Proc. of American Control Conference*, 1990.
- [18] G. E. Forsythe, M. A. Malcolm, and C. B. Moler, *Computer Methods for Mathematical Computations*, Prentice-Hall, 1976.
- [19] N. Qaiser, A. Hussain, N. Iqbal, and N. Qaiser, "Dynamic surface control for stabilization of the oscillating eccentric rotor," *Proc. IMechE Part I: Journal of Systems and Control Engineering*, vol. 221, no. 3, pp. 311-319, 2007.
- [20] M. Jankovic, D. Fontaine, and P. V. Kokotovic, "TORA example: Cascade and passivity based control designs," *IEEE Trans. on Control System Technology*, vol. 34, no. 7, pp. 907-915, 1996.
- [21] M. W. Spong, "The swing up control problem for the Acrobot," *IEEE Control Systems Magazine*, vol. 15, no. 1, pp. 49-55, Feb. 1995.



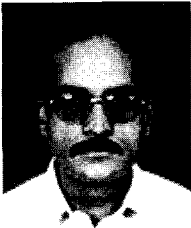
Nadeem Qaiser graduated with a B. Eng in Electronics in 1989, from NED University of Engineering and Technology, in Karachi, Pakistan. For 1999-2001, he worked as a Research Fellow at the FINUDA Experiment at Italian National Physics Research Laboratories LNF/INF, Frascati (Rome) Italy. He is engaged in Ph.D.

degree at Pakistan Institute of Engineering and Applied Sciences Pakistan. His Ph.D. research is about study of Non-linear Dynamical System Modeling & Control.



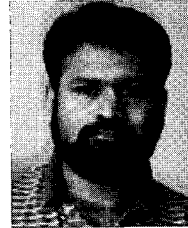
Amir Hussain graduated with in 1992, from the University of Strathclyde in Glasgow, UK. He was awarded the Ph.D. degree in 1996 and the thesis was titled "Novel Artificial Neural-Network Architectures & Algorithms for Non-linear Dynamical System Modeling & Digital Communications Applications". Since 2000, he is

working as an Academic Staff Member at the University of Sterling, Scotland, UK, where he is researching as part of the multi-disciplinary research Centre for Cognitive & Computational Neuroscience (CCCN).



Naeem Iqbal graduated with a B.Sc. in Electrical Engineering from N-W.F.P. University of Engineering and Technology Peshawar on 1989. He received the Ph.D. degree from University of Rennes France in December 1997, entitled "Invariance and suboptimal control of implicit large scale system using hybrid dynamic systems

approach". He recently completed his Post Doctorate Work in Hashimoto Lab, Tohoku University, Sendai, Japan. He has been Head of Department of Electrical Engineering, Pakistan Institute of Engineering and Applied Sciences and has been involved in teaching various subjects of control systems engineering and industrial automation with research work focused around control systems.



Naeem Qaiser mastered in Electronic in 1993, from Qaid-e-Azam University Islamabad, Pakistan. Later on he received the M.S. degree in Systems Engineering from the same University in 1997. He then worked as an Electronics Design Engineer in Electronics Laboratories NESCOM, Islamabad, Pakistan. He was awarded

PhD merit scholarship and has been working since as Doctorate Scholar at Pakistan Institute of Engineering and Applied Sciences Pakistan. His interests also include visual control systems.